Variable-Frequency Explicit Model Predictive Control of Wide Band Gap DC/DC Converter with Critical Soft Switching

Liwei Zhou and Matthias Preindl
Department of Electrical Engineering, Columbia University in the City of New York
New York City, NY, USA

Abstract− This research proposes a control scheme that ensures critical soft switching to improve the efficiency and power density of the DC/DC power converter. First, we analyze the boundary constraints of critical soft switching that are derived with the key parameters of the interlock time and threshold current for typical SiC and GaN devices. Then, a variable-frequency model predictive control strategy is proposed for synchronous DC/DC converters. The duty cycle and frequency are controlled by MPC to satisfy the critical soft switching constraints in every operating point. The explicit model predictive control method can be applied to increase the speed of optimization. The combination of Explicit Model Predictive Control (EMPC) and critical soft switching technique largely improves the efficiency and tracking accuracy of the system. Also due to the fast response of the MPC, the losses during the transient period can be further reduced without oscillation compared to the traditional PI controller. Finally, the theoretical analysis is validated by dedicated tests.

I. INTRODUCTION

The wide band gap devices, SiC and GaN, are becoming more and more popular in the application of power converters due to the high frequency. To improve the power density of the system, small size of passive devices and high frequency are two main points to be considered when designing the DC/DC converter. [1-2] However due to the large ripple current, the power losses should be paid more attention when reducing the size of inductor. [3] A critical soft switching method is proposed in this paper to achieve zero voltage turn-on with pre-designed peak/valley inductor current threshold and dead time. The critical soft switching constraints are calculated accurately according to the data sheet to control the peak/valley inductor current operating in the feasible soft switching regions. Also, a variable-frequency model predictive control method is proposed to implement the critical soft switching constraints. [4-5] The combination of critical soft switching technique and model predictive control method can reduce the power losses especially during the transient period because of the fast response of MPC. Compared with the traditional PI controller, the proposed method can track the reference faster without oscillation, thus the critical soft switching operation will be maintained even during the transient period.

Some research has published the work of ZVS in DC/DC converters by applying a negative inductor current. [6-9] But the detailed boundary conditions of soft switching have not been analyzed. This paper derives the critical soft switching conditions in function of dead time and peak/valley inductor current. And a variable-frequency model predictive control method is proposed with the combination of critical soft switching technique and explicit MPC. The paper is organized as follow. Firstly, the boundaries of critical soft switching constraints for DC/DC converter are derived with dead time and peak/valley inductor current by data sheet and integral equations. Secondly, the variable-frequency model predictive method is introduced with the proposed critical soft switching constraints. The explicit MPC method can be applied to the

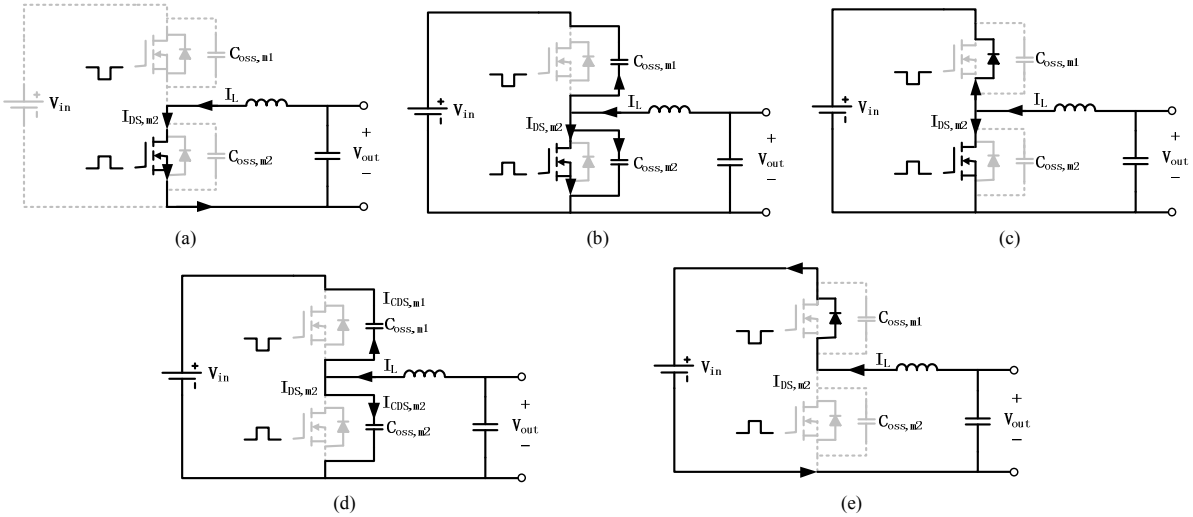

Fig. 1. The charging and discharging processes of SiC DC/DC converter during the switching transition period of negative inductor current.

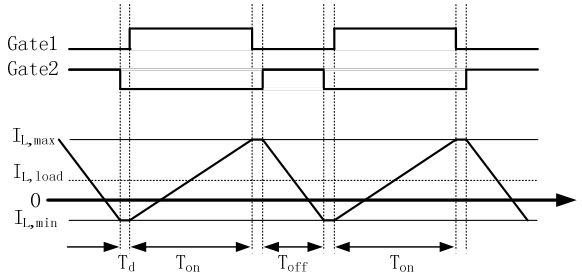

Fig. 2. Gate signals and inductor current for critical soft switching.

implementation to increase the speed of optimization process. The power losses can be largely reduced during the transient period. Finally, the rigorous test procedures verify the theoretical analysis.

II. CRITICAL SOFT SWITCHING PRINCIPLES FOR DC/DC CONVERTER

In this section, the critical soft switching technique is introduced with the derived boundary conditions of dead time and peak/valley inductor current by datasheet and integral equations. The main purpose of the critical soft switching method is to replace the large turn-on loss of upper switch with small turn-off loss of lower switch.

Fig. 1 shows the circuit of SiC DC/DC converter with the equivalent input and output capacitors in different working conditions during the dead time. It illustrates the charging and discharging processes during the switching transition period when the inductor current reaches the minimum negative point. From Fig. 1(a) to Fig. 1(f), the different current flowing paths during lower switch turn-off period are illustrated step by step. With the charging capability of negative inductor current for the upper switch output capacitor, the turn-on loss of the upper switch can be replaced by the turn-off loss of the lower switch. For the critical soft switching, a large current ripple is required to ensure negative valley inductor current to be lower than a threshold current level as is shown in Fig. 2. In the turn-off transient period of lower switch, the negative inductor current will discharge the upper switch output capacitor, $C_{oss,m1}$, as is shown in Fig. 1(b)-(d). The ZVS of upper switch can be achieved if the $C_{oss,m1}$ is fully discharged before it turns on. The ZVS operation depends on the interlock time between two switches and the value of inductor valley current. According to Fig. 1, the inductor valley current can be expressed as:

$$I_{L,\min} = I_{DS,M2} + I_{\text{coss},M1} + I_{\text{coss},M2} \tag{1}$$

where $I_{DS,M1/2}$ is the drain current, $I_{coss,M1/2}$ is the current through the switch output capacitance, C_{oss}. Because

$$I_{\text{coss},M1(2)} = \mathrm{C}_{\text{oss},M1(2)} \cdot \frac{dU_{DS,M1(2)}}{dt} \tag{2}$$

And ($U_{DS,M1}$+$U_{DS,M2}$) equals to the input source voltage, U_{in}, which is a constant value, then $I_{l,min}$ can be expressed as:

$$\begin{aligned} I_{L,\min} &= I_{DS,\mathrm{M2}} + (\mathrm{C}_{\text{oss},M1} + \mathrm{C}_{\text{oss},M2}) \cdot \frac{dU_{DS,M2}}{dt} \\ &= I_{DS,\mathrm{M2}} - (\mathrm{C}_{\text{oss},M1} + \mathrm{C}_{\text{oss},M2}) \cdot \frac{dU_{DS,M1}}{dt} \end{aligned} \tag{3}$$

Similarly, the maximum positive value of inductor current is:

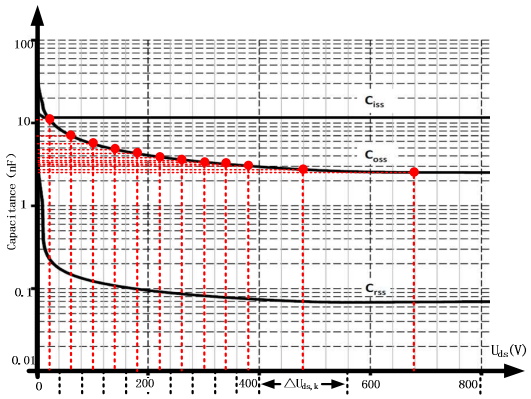

Fig. 3. The traced points of output capacitance with U_{ds}.

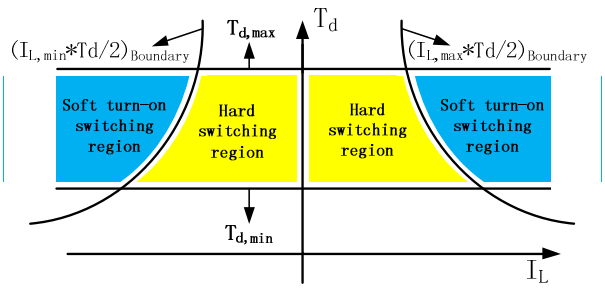

Fig. 4. Boundary conditions for critical soft switching regions.

$$I_{L,\max} = I_{DS,\mathrm{M1}} + (\mathrm{C}_{\text{oss},M1} + \mathrm{C}_{\text{oss},M2}) \cdot \frac{dU_{DS,M2}}{dt} \tag{4}$$

The above current equations can be further analyzed by the integral calculation over time and U_{ds}, respectively.

$$\begin{aligned} &\int_0^{T_d} \left[I_{L,\min} - I_{DS,\mathrm{M2}}(\mathrm{t}) \right] dt \\ &= \int_0^{U_{in}} \left[\mathrm{C}_{\text{oss},M1}(U_{DS,M2}) + \mathrm{C}_{\text{oss},M2}(U_{DS,M2}) \right] dU_{DS,M2} \\ &\int_0^{T_d} \left[I_{L,\max} - I_{DS,\mathrm{M1}}(\mathrm{t}) \right] dt \\ &= \int_{U_{in}}^{0} \left[\mathrm{C}_{\text{oss},M1}(U_{DS,M2}) + \mathrm{C}_{\text{oss},M2}(U_{DS,M2}) \right] dU_{DS,M2} \end{aligned} \tag{5}$$

For simplification, Ids can be assumed to be varying linearly with time. Then the left side of the above two equations in (5) can be calculated as:

$$\begin{aligned} &\int_0^{T_d} \left[I_{L,\min} - I_{DS,\mathrm{M2}}(\mathrm{t}) \right] dt \\ &= \int_0^{T_d} \left[I_{L,\min} - (I_{L,\min} - \frac{I_{L,\min}}{T_d} t) \right] dt = \frac{1}{2} I_{L,\min} T_d \\ &\int_0^{T_d} \left[I_{L,\max} - I_{DS,\mathrm{M1}}(\mathrm{t}) \right] dt \\ &= \int_0^{T_d} \left[I_{L,\max} - (I_{L,\max} - \frac{I_{L,\max}}{T_d} t) \right] dt = \frac{1}{2} I_{L,\max} T_d \end{aligned} \tag{6}$$

So, the critical soft switching inequalities of $I_{L,min(max)}$ and T_d can be expressed as:

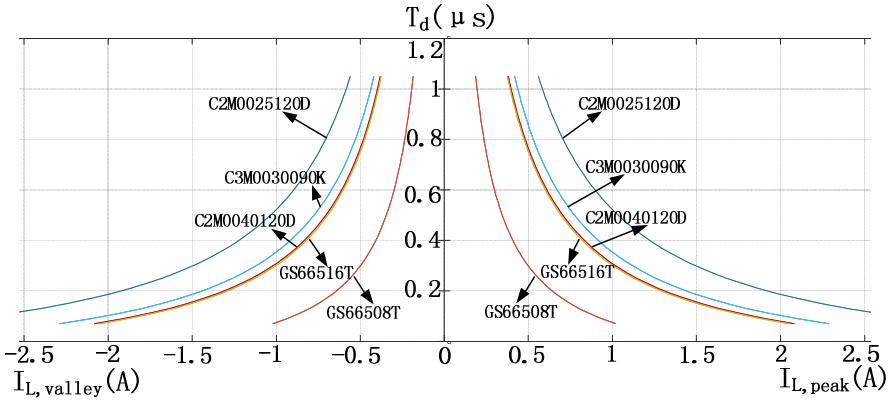

Fig. 5. The soft switching operation regions for different devices.

$$\frac{1}{2}I_{L,\min}T_d \le \int_0^{U_{in}}\left[C_{oss,M1}(U_{DS,M2})+C_{oss,M2}(U_{DS,M2})\right]dU_{DS,M2}$$
$$\frac{1}{2}I_{L,\max}T_d \ge \int_{U_{in}}^{0}\left[C_{oss,M1}(U_{DS,M2})+C_{oss,M2}(U_{DS,M2})\right]dU_{DS,M2} \quad (7)$$

Thus the minimum negative and maximum positive inductor current can be derived with the variables of dead time, Td, and the integration of output capacitors with drain-source voltages. The design of the converter should satisfy the two inequalities to make sure the critical soft switching operation. The integration of switch output capacitance with drain-source voltages can be calculated by the datasheet provided by the manufacturer. Fig. 3 shows the relationship of output capacitance with drain-source voltages under the specific testing condition (T_j=25°C, V_{AC}=25mV, f=1MHz). So the integrations of (7) can be calculated by tracing several discrete voltage intervals multiplied by the corresponding capacitance value and then accumulate together. Because the sum of voltages across switch M1 and M2 are constant and equal to U_{in}, so their integration of output capacitance with drain-source voltages are identical during the integral limits from 0 to U_{in} and U_{in} to 0, respectively. Then, only one switch integration is needed to be calculated. According to Fig. 3, the right side of (7) can be derived by tracing n points on the curve of C_{oss} and summing up the n intervals together:

$$\int_0^{U_{in}}\left[C_{oss,M1}(U_{DS,M2})+C_{oss,M2}(U_{DS,M2})\right]dU_{DS,M2} \approx 2\sum_{k=1}^{n}C_{oss,M2}(U_{DS,M2k})\Delta U_{DS,M2k} \quad (8)$$

Then, the model of critical soft-switching method can be expressed with the function image in Fig. 4. It can be shown that the blue regions are the feasible soft switching range according to the constraints of (7) with the maximum and minimum dead time requirement. Also, the soft switching ranges of typical GaN and SiC devices are given in Fig. 5. During controlling part in the following sections, the dead time and peak/valley inductor current can be controlled within the critical soft switching region for the converter.

III. MODEL PREDICTIVE CONTROLLER

The proposed variable-frequency model predictive controller is introduced in this section. For the purpose of controlling the peak/valley inductor current in the critical soft switching regions, the duty cycle and frequency are set to be the two input values in the model predictive model. Because the duty cycle and frequency have strong coupling relationship in the discrete state equation, a new input value is defined to replace the duty cycle.

A. System Model

The model of the DC/DC converter can be expressed as:

$$L\frac{di_L(t)}{dt} = d(t)\cdot U_{in} - u_{out}(t)$$
$$C\frac{du_{out}(t)}{dt} = i_L(t) - i_{out}(t) \quad (9)$$

To discretize the state equations:

$$i_L(k+1) = i_L(k) + \frac{U_{in}\cdot d(k)\cdot T_s(k)}{L} - \frac{u_{out}(k)\cdot T_s(k)}{L}$$
$$u_{out}(k+1) = u_{out}(k) + \frac{i_L(k)\cdot T_s(k)}{C} - \frac{i_o(k)\cdot T_s(k)}{C} \quad (10)$$

From (10), it can be seen that the input values of duty cycle and time period is coupled which causes the nonlinear problem and is hard to solve for MPC implementation. To eliminate the coupled terms of duty cycle and time period, the new state value of $d(k)T_s(k)$ is set as D(k), then the vector of input value is [D(t), T_s(t)], the first state equation of (10) can then be expressed as:

$$i_L(k+1) = i_L(k) + \frac{U_{in}\cdot D(t)}{L} - \frac{u_{out}(k)\cdot T_s(k)}{L} \quad (11)$$

From the derived state equation of (11), another problem is the bilinear term of output voltage and time period which is not feasible for explicit MPC optimization. For the purpose of solving the coupled term of output voltage and time period, a cascaded controlling method is proposed. The output voltage is firstly controlled by a PI controller which will provide the current reference for the MPC operation. So the controlling part includes two cascaded stages: the first stage of PI control for output voltage and the second stage of MPC control for inductor current. Then the output voltage can be approximately regarded as fixed and will not influence the iteration of current control. The new decoupled state equation for the MPC implementation can be finally updated as:

$$i_L(k+1) = i_L(k) + \frac{U_{in}\cdot D(t)}{L} - \frac{U_{out}\cdot T_s(k)}{L} \quad (12)$$

So the state value, X_k, input value, U_k, parametric matrix, A

and B for the discrete state equation can be expressed as:

$$X_k = i_L(k)\text{-}i_{Lr}(k);$$
$$U_k = [d(k)\cdot T_s(k);\ T_s(k)] = [D(k);\ T_s(k)] \quad (13)$$
$$A = [1];\ B = \left[\frac{U_{in}}{L},\ -\frac{U_{out}}{L}\right]$$

B. MPC Formulation

(1) Cost Function:

The main goal of the model predictive controller is to track the inductor current as reference and minimize the error. [10-11] Also, the time period (frequency) can be added into the cost function to maximize the frequency in the region of critical soft switching operation. So the cost function of MPC can include two terms: first one is the minimization of current tracking error, second term is the maximization of frequency in the region of soft switching operation.

$$\min \quad \sum_{k=0}^{N} (X_k^T Q X_k + U_k^T R U_k) \quad (14)$$

where N is the predictive horizon, Q is [q] and R is [0, 0; 0, r]. (q and r represent the weight between the two terms in the cost function)

(2) Critical Soft Switching Constraints

The critical soft switching operation can be achieved by implementing the constraints on the state value, $i_L(k)$, and the input value, [D(k); $T_s(k)$]. The constraints include four parts: firstly, the time period should be within the range of [$T_{s,min}$, T_{smax}] according to the sampling and dead time requirements; secondly, the range of duty cycle is [0, 1]; thirdly, the peak/valley inductor current should be higher/lower than the threshold current, I_{th}, which has been derived in section II; finally, the peak/valley inductor current should be lower/higher than the maximum device current, I_{max}, which can be derived by the datasheet. Thus, the constraints can be linearly expressed as:

$$s.t. \quad T_{s,\min} \le T_s(k) \le T_{s,\max}$$
$$0 \le d(k) \le 1$$
$$\Rightarrow 0 \le D(k) \le T_s(k)$$
$$\begin{cases} -I_{\max} \le i_L(k) - \dfrac{\Delta i_L}{2} \le -I_{th} \\ I_{th} \le i_L(k) + \dfrac{\Delta i_L}{2} \le I_{\max} \end{cases}$$
$$\Rightarrow \begin{cases} -I_{\max} \le i_L(k) - \dfrac{U_{in} - U_{out}}{2L}\cdot D(k) \le -I_{th} \\ I_{th} \le i_L(k) + \dfrac{U_{in} - U_{out}}{2L}\cdot D(k) \le I_{\max} \end{cases} \quad (15)$$

The constraints in (15) are linear for all the state and input variables. Thus the requirements of explicit model predictive controller can be satisfied. And the function of operating within the critical soft switching regions to reduce the switching losses will also be achieved with fast offline calculation.

(3) Implementation

The operating trajectories of the proposed model predictive controller can be illustrated in Fig. 6. The inductor current can be varying according to the reference. The proposed MPC controller will track the reference current to achieve the critical soft switching by the constraints. Meanwhile the maximum frequency will be realized because the frequency term has been added to the cost function in (14). So the

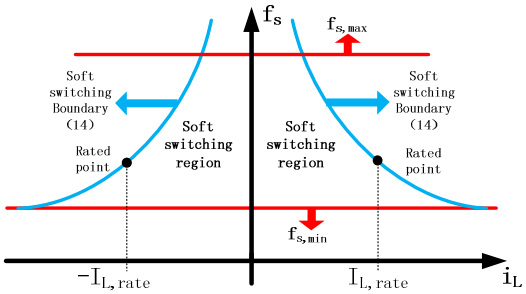

Fig. 6. The operating trajectories of MPC method.

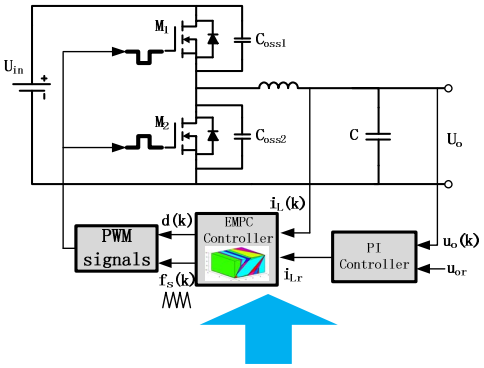

Algorithm
do at each sampling instant,
Step1: measure $u_o(k)$ and $i_L(k)$.
Step2: derive current reference, $i_{Lr}(k)$ from PI.
Step3: derive optimal U(k)* from EMPC
Step4: apply first term of U* to the switches.
Step5: wait for the next sampling instant (k+1).
enddo

Fig. 7. Controlling blocks and algorithm.

operating trajectories will be around the soft switching boundaries which can be derived by the function of frequency and average current (blue lines in Fig. 6):

$$f_s = \begin{cases} \dfrac{(1-d)\cdot d\cdot U_s}{2\cdot(\bar{i}_L + I_{th})\cdot L}, & i_L \ge 0 \\ \dfrac{(1-d)\cdot d\cdot U_s}{2\cdot(I_{th} - \bar{i}_L)\cdot L}, & i_L \le 0 \end{cases} \quad (16)$$

Also the controlling blocks are shown in Fig. 7 which follows the algorithm in every sampling instant. For the explicit model predictive, one of the advantages is the fast calculation speed because of an offline formulation of state equation parameters in high frequency operation. [8] [12] The cost function in (14) is quadratic and the derived critical soft switching constraint in (15) is affine. Thus, the close-loop controlling regions are piecewise linear. According to the implementation of the explicit model predictive control method, a search-tree can be computed and formulated for the online tracking. The combination of piecewise linear feedback laws and search tree will largely reduce the calculation complexity of online optimization in traditional MPC process. So for the high frequency application, the proposed explicit model predictive control method can be speed up and satisfy

the sampling requirement. [13]

IV. RESULTS

The variable-frequency model predictive control is implemented in this section based on a typical SiC device, C2M0025120D by rigorous testing procedure. The circuit parameters are: input voltage 800V, output voltage 400V, inductor 10uH, operation time 4ms. Fig. 8(a) and (b) show the comparison of the key waveforms between the proposed method and the traditional PI controller with the same current reference step (from 10A to 20A) triggered in the middle of the operating period. Specifically, the inductor current, sampling current, duty cycle and time period are given in each plot. As is shown in Fig. 8(a), the critical soft switching constraints can be satisfied in all the operation time including the transient period. However, the traditional PI controller cannot guarantee the critical soft switching during the transient period because of the oscillation. So the proposed variable-frequency model predictive control method can further reduce the power losses.

V. CONCLUSION

This paper proposes a variable-frequency explicit model predictive control method for DC/DC converter with the combination of critical soft switching and variable-frequency EMPC. The precise critical soft switching boundaries for DC/DC converter are derived with the parameters of dead time and peak/valley inductor threshold current. The dynamic system of the variable-frequency state equation is analyzed. Also the constraints of critical soft switching are added to the proposed model predictive controller. The proposed method solves the problem of turn-on power losses during the transient period which further improves the efficiency compared to the traditional PI controller. The results verify the validity of the theoretical analysis.

VI. ACKNOWLEDGEMENT

This research is based in part upon work supported by National Science Foundation under Grant Number 1653574.

REFERENCES

[1] C. Xiao, G. Chen, and W. G. Odendaal, "Overview of Power Loss Measurement Techniques in Power Electronics Systems," IEEE Transactions on Industry Applications, vol. 43, no. 3, pp. 657–664, 2007.

[2] Y. Rao, S. P. Singh, and T. Kazama, "A Practical Switching Time Model for Synchronous Buck Converters," Proc. IEEE Applied Power Electronics Conference and Exposition, Long Beach, CA, pp. 1585–1590, 2016.

[3] Y. Ren, M. Xu, J. Zhou, and F. C. Lee, "Analytical Loss Model of Power MOSFET," IEEE Transactions on Power Electronics, vol. 21, no. 2, pp. 310–319, 2006.

[4] J. Rodriguez, J. Pontt, C. A. Silva, P. Correa, P. Lezana, P. Cortes, and U. Ammann, "Predictive current control of a voltage source inverter," IEEE Trans. Ind. Electron., vol. 54, p. 495503, 2007.

[5] A. Bemporad, M. Morari, V. Dua, and E. N. Pistikopoulos, "The explicit solution of model predictive control via multiparametric quadratic programming," in ACC, 2000.

[6] M. Preindl, E. Schaltz, and P. Thogersen, "Switching frequency reduction using model predictive direct current control for high-power voltage source inverters," IEEE Trans. Ind. Electron., vol. 58, no. 7, pp. 2826– 2835, 2011.

[7] S. Bolognani, S. Bolognani, L. Peretti, and M. Zigliotto, "Design and implementation of model predictive control for electrical motor drives," IEEE Trans. Ind. Electron., vol. 36, pp. 1925–1936, 2009.

[8] S. Mariethoz and M. Morari, "Explicit model predictive control of a PWM inverter with an LCL filter," IEEE Trans. Ind. Electron., vol. 56, no. 2, pp. 389–399, 2009.

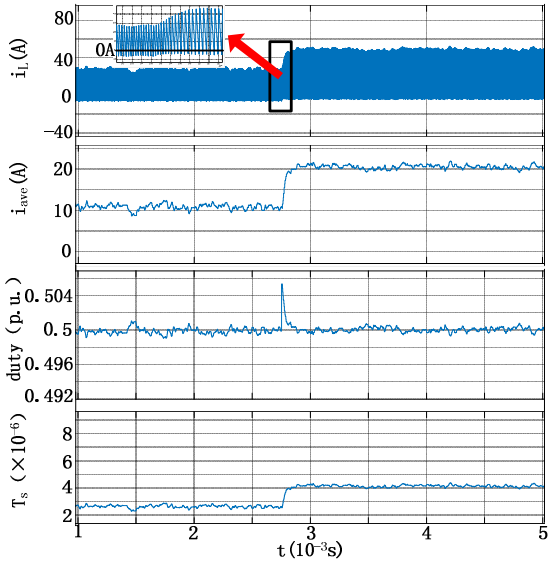

(a)

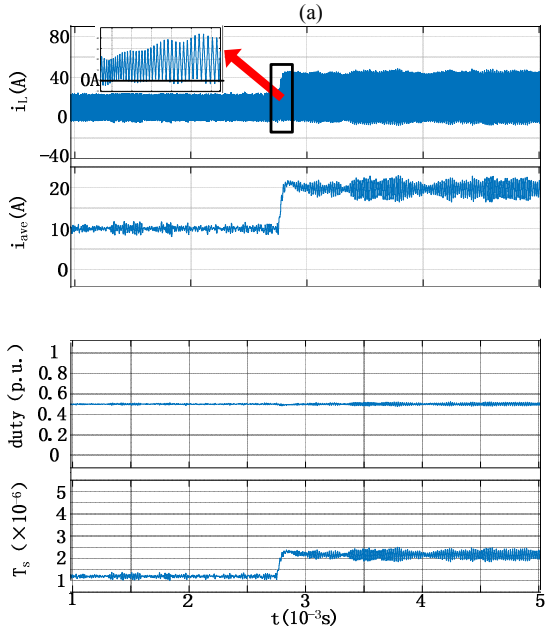

(b)

Fig. 8. The key waveforms of inductor current, duty cycle, time period between (a) proposed MPC method and (b) PI.

[9] S. Kouro, P. Cortes, R. Vargas, U. Ammann, and J. Rodríguez, "Model predictive control—A simple and powerful method to control power converters," IEEE Trans. Ind. Electron., vol. 56, no. 6, pp. 1826–1838, 2009.

[10] S. Vazquez, C. Montero, C. Bordons, and L. Franquelo, "Model predictive control of a VSI with long prediction horizon," in Proc. 2011 IEEE Int. Symp. Industrial Electronics (ISIE), 2011, pp. 1805–1810.

[11] Z. Song, C. Xia, and T. Liu, "Predictive current control of three-phase grid-connected converters with constant switching frequency for wind energy systems," IEEE Trans. Ind. Electron., vol. 60, no. 6, pp. 2451–2464, 2013.

[12] P. Cortes, J. Rodríguez, D. Quevedo, and C. Silva, "Predictive current control strategy with imposed load current spectrum," IEEE Trans. Power Electron., vol. 23, no. 2, pp. 612– 618, 2008.

[13] R. Vargas, P. Cortes, U. Ammann, J. Rodríguez, and J. Pontt, "Predictive control of a three-phase neutral-point-clamped inverter," IEEE Trans. Ind. Electron., vol. 54, no. 5, pp. 2697–2705, 2007.